Development and thermal characteristics of a novel composite oleic acid for cold storage

L. Jiang[a,b,*], R.Z. Wang[b], A.P. Roskilly[a]

[a] *Sir Joseph Swan Centre for Energy Research, Newcastle University, Newcastle NE1 7RU, UK*

[b] *Institute of Refrigeration and Cryogenics, Shanghai Jiao Tong University, Shanghai, 200240, China*

Abstract: This paper presents a novel composite material for cold storage. Oleic acid is selected as phase change material whereas carbon coated aluminum is adopted as additive. Thermal conductivities and viscosities of samples are investigated by light flash method and viscometer. Phase change temperature and latent heat are analyzed through DSC measurements. It is indicated that thermal conductivities of composite oleic acid using nanoparticles are remarkably improved when compared with pure sample. The highest thermal conductivity of composite oleic acid with 1 wt% mass ratio of Al@C could reach 0.42 $W \cdot m^{-1} \cdot K^{-1}$, which is 2 times higher than that of pure oleic acid. When testing temperature increases from 25°C to 75°C, dynamic viscosities decrease from 3.67 mPa·s to 1.062 mPa·s. Phase change temperature and latent heat are slightly shifted from that of pure oleic acid. This novel composite oleic acid reveals vast potentials to stabilize the performance of solar sorption cooling system.

Keywords: Oleic acid, Carbon coated aluminum, Thermal conductivity, Solar sorption

* This paper is a substantial extension of short version of the conference paper presented at the 6th International Conference on cryogenics Refrigeration (ICCR2018) on April 12-14, Shanghai, China. Original paper title 'Development and thermal characteristics of a novel composite oleic acid for cold storage'.
* Corresponding author. Tel. +44-07592206270
Email: Long.jiang@newcastle.ac.uk (L. Jiang)

Nomenclature

A	Pre-experimental factor (Pa·s)
AC	Activated carbon
Al@C	Carbon coated aluminum
C	Specific heat ($J \cdot g^{-1} \cdot K^{-1}$)
CNT	Carbon nanotube
DSC	Differential scanning calorimeter
d	Thickness of sample (mm)
E	Activation energy ($kJ \cdot mol^{-1}$)
ENG	Expanded natural graphite
HTF	Heat transfer fluid
h	Heat transfer coefficient ($W \cdot m^{-2} \cdot K^{-1}$)
L	Length of cold storage unit (m)
LTES	Latent thermal energy storage
PCM	Phase change material
R	Universal gas constant ($J \cdot mol^{-1} \cdot K^{-1}$)
S	Superficial capsule area (m^2)
STES	Sensible thermal energy storage
T	Temperature (°C)
TES	Thermal energy storage
t_{50}	Half time (s)
u	Mean velocity ($m \cdot s^{-1}$)

Greek letters

α	Thermal diffusivity ($mm^2 \cdot s^{-1}$)
β	Mass ratio of oleic acid
λ	Thermal conductivity ($W \cdot m^{-1} \cdot K^{-1}$)
ε	Void fraction
ρ	Density ($g \cdot cm^{-3}$)
μ	Dynamic viscosity (mPa·s)

ΔH	Phase change enthalpy ($kJ \cdot kg^{-1}$)

Subscripts

Al@C	Carbon coated aluminum
com	Composite PCM
f	Fluid
in	Inlet
ini	Initial
ole	Oleic acid
R	Radius of capsule

1. Introduction

With regard to the imbalance between energy demand and supply, thermal energy storage (TES) has been becoming one of the key technologies for renewable energy utilization and industrial waste heat recovery (Miró et al., 2016). As one method of TES, latent thermal energy storage (LTES) is gathering the momentum. This is mainly because it has high energy storage density with a small temperature difference when comparing with sensible thermal energy storage (STES) (Veerakumar and Sreekumar, 2016). Also it enjoys a higher thermal stability than thermochemical energy storage in terms of energy output (Yu et al., 2013). Heat storage materials with relatively high phase change temperatures are widely investigated (Merlin et al., 2016). Comparably, cold storage materials are less studied since selection of phase change materials (PCMs) could be limited. By using PCMs for cold storage, it could release the cooling effect to reduce the peak electric power for air conditioning (Li et al., 2012).

It is extensively acknowledged that solar sorption cooling technology is another hot topic in recent years due to its characteristics, e.g. simple structure, environmental friendliness and wide availability (Wang et al., 2016). Nonetheless, cooling output of the system cannot be stabilized since solar energy is featured as intermittent and periodic heat source (Zhao et al., 2018). Thus the mismatch between cold output of sorption chiller and cooling demand of user becomes a barrier to the commercialization of this green technology (Pan and Wang, 2018). A feasible solution is solar sorption system integrated with cold storage unit, which could stabilize the cooling output (Al-Alili et al., 2014). A classical design of high temperature solar cooling application is the integration of cooling system with radiant cooling terminals (Pantelic et al., 2018). Another design is packed bed which has been analysed

extensively due to its simple structure, large surface area and good thermal transport property (Cheng et al., 2016). Chilled water supplied to high temperature cooling terminal is usually in the range from 15ºC to 19ºC (Zhao et al., 2014). Given that phase change temperature should be a bit lower, it is between 13ºC and 15ºC (Oró et al., 2012). Comparably, chilled water temperature of a conventional air-conditioning system is usually about 7ºC. Then the applied cold storage PCMs should have low phase change temperatures of around 5ºC. But quite few material could be directly selected in this temperature range when considering safety, causticity, flammability and cost. Organic eutectic e.g. capric and lauric acid with oleic acid as additive is a choice of cold storage material for solar cooling due to its low phase change temperature which could be adjusted by using different mass proportions (Zhai et al., 2013). But organic PCMs usually have relatively low thermal conductivities (Atinafu et al., 2018). Thus heat transfer enhancement of PCMs is always one of research highlights for real application of cold storage.

Various methods are attempted to improve thermal transport properties of PCMs for cold storage (Sidik et al., 2018). A common way is to incorporate highly conductive materials, and carbon–based and metal–based types are two main additives (Lin et al., 2018). Carbon–based additives e.g. expanded natural graphite (ENG), carbon fibre have high thermal conductivities, stable thermal and good compatibility. However, their developments sometimes have a few challenges. Metal–based additives e.g. metal foam are also quite conducive to thermal conductivity enhancement. Also some restrictions happen when considering the real applications e.g. unstable heat transfer due to the various dispersions (Oró et al., 2012). Then nanoparticles are introduced to PCMs for improved thermal conductivities, which are followed by the concept of nanofluids. Kumaresan et al. (Chandrasekaran et al., 2014b; Kumaresan et al., 2013) investigated the nanofluid PCM by dispersing the multi-wall carbon nanotubes (CNT) with de-ionized water. It was demonstrated that solidification time could be reduced by 20% with nanofluid PCM. Later, their research team studied water dispersed with graphene nanoplatelets. Results indicated that the maximum thermal conductivity enhancement of 56% was obtained (Sathishkumar et al., 2016). Besides, another nanoparticles of metal oxides e.g. Al_2O_3, CuO, MgO and TiO_2 are investigated to intensify thermal conductivities of PCMs (Altohamy et al., 2015; Chandrasekaran et al., 2014a). Studies showed that even a small fraction of metallic oxides could favorably increase thermal conductivity of pure substances (Chandrasekar et al., 2010; Fang et al., 2013). Although thermal conductivity of base material is increased, heat capacity is correspondingly increased. Then activated carbon nanosheet is expected to be a tertiary additive into composite cold storage material using metal oxides (Hussain et al., 2017). Compared with the former two type nanoparticles, carbon coated metal is a combination of their advantages, which has been verified to be conducive to the kinetics of

sorbents (Jiang et al., 2017). Also it has a good compatibility and stability when mixing with diesel fuel (Jiang et al., 2018). Carbon coating protects external conditions for metal inside with excellent thermo-physical properties remained. It tends to imagine that carbon coated metal could be selected to integrate with PCMs for cold storage, which may also have a positive influence on its heat transfer performance. It is recognised that viscosity is another significant index for evaluating cold storage PCMs which is often experimental tested and simulated by some empirical equations (Barreneche et al., 2017). Nanoparticles are attempted to be selected to improve its physical performance in the working temperature range. Eyring equation is used for further assessing the activation energy of PCMs, which could analyze the roles of nanoparticles (Han et al., 2010).

Under this scenario, this paper aims to investigate thermal transport properties of composite oleic acid by using carbon coated aluminum (Al@C) as the additive, which is the first time to be applied for cold storage PCM in terms of various mass proportions. Also viscosity is expected to be improved by using this nanoparticles. Variations of phase change temperature and latent heat are indicated by differential scanning calorimeter (DSC) testing. PCM capsules are adopted to fill a cold storage unit. Based on the performance of a selected solar sorption refrigerator, cold storage unit is then simulated for its cooling output, which is compared with experimental results with regard to thermal stability of heat transfer fluid (HTF). Also the unit with PCM using and not using Al@C are also compared to illustrate the role of carbon nanoparticles.

2. Material and development

Composite oleic acid is developed by using Al@C with different mass ratios i.e. 0.25 wt%, 0.5 wt% and 1 wt%. The developing process is shown in Fig. 1a, which is described as follows: Al@C is first heated for removing its water inside (a1 process). Simultaneously, oleic acid is measured as a set volume (a2 process). Then the mixture is combined with oleic acid in ultrasonic bath for 2 hours (b process). The frequency is controlled as 60 Hz. This process aims to fully disperse the aggregated particles and have a good distribution in oleic acid. After that, liquid sample becomes darker, which indicates a homogeneous distribution in oleic acid (c process). Finally, composites are poured into small bottles to observe the precipitation. Fig. 1b indicates the photos of composite samples with different mass ratios of Al@C and pure sample. It could be observed that Al@C is well mixed in composite material due to the fact that Van der Waals force of Al@C is stronger than its gravity. Thus it is recommended that mass ratio of Al@C is not higher than 5%, otherwise it will deposit after a while. It is predictable that the composite PCM is not corrosive by physical mixing two components.

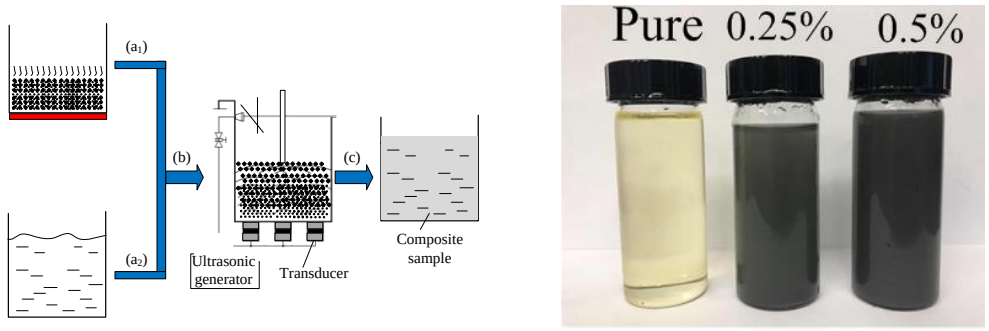

(a) (b)

Fig. 1. Development of composite oleic acid (a) schematic; (b) photo of materials.

3. Testing methodology

Thermal conductivity of composite oleic acid is investigated by light flash method, and the concerning testing equipment, i.e. LFA467 instrument. Structure and testing procedures of the unit could refer to the reference (Jiang et al., 2014). The testing temperature is monitored by means of an infrared detector, which should be initially calibrated by liquid nitrogen before testing. Thermal diffusivity is determined through the curve of temperature vs. time. Sample holder for liquids is specially adopted in the experiment which is shown in Fig. 2. The liquid is filled into the holder by using 1 mm syringe and then the hole is blocked by locking pins.

Heat conduction of testing sample is considered to be one-dimensional heat transfer process due to infinitely small width of optical pulse. Thermal diffusivity is evaluated by equation 1:

$$\alpha = 0.1388 \cdot d^2 / t_{50} \tag{1}$$

where α is thermal diffusivity ($mm^2 \cdot s^{-1}$), d is thickness of testing sample (mm), t_{50} is semi-heating time (s).

Thermal conductivity is then calculated by equation 2:

$$\lambda = \rho(T) \cdot C_p(T) \cdot \alpha(T) \tag{2}$$

where $\lambda(T)$ is thermal conductivity at a testing temperature ($W \cdot m^{-1} \cdot K^{-1}$), $\alpha(T)$ is thermal diffusivity ($mm^2 \cdot s^{-1}$), C_p is specific heat ($J \cdot g^{-1} \cdot K^{-1}$), $\rho(T)$ is density of the sample ($g \cdot cm^{-3}$).

Specific heat and density of novel composite oleic acid are calculated by equation 3 and 4, which are according to their respective mass ratios of mixture.

$$\rho_{com} = \beta \cdot \rho_{p,ole} + (1 - \beta) \cdot \rho_{p,Al@C} \tag{3}$$

$$C_{p,com} = \beta \cdot C_{p,ole} + (1 - \beta) \cdot C_{p,Al@C} \tag{4}$$

where β is mass ratio of oleic acid with respect to total mass of novel composites.

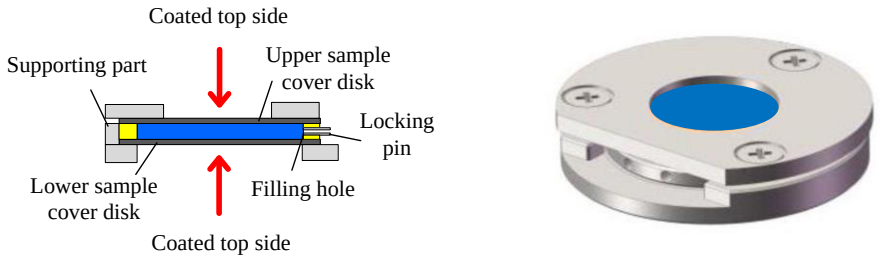

Fig. 2. Sample holder for low-viscous liquid (a) schematic; (b) photo (Jiang et al., 2014).

The onset temperature and phase change heat are tested by DSC 214 equipment which is also produced by NETZSCH under nitrogen atmosphere at a constant flow rate of 50 ml·min^{-1}. For each temperature, the degree of accuracy is up to ±0.05°C. The precision of DSC is less than ±0.01%. The heating/cooling rate is set at 1 K·min^{-1}. The liquid is filled into the sample holder by using syringe and then sealed with a lid.

4. Testing results and discussions

4.1. Thermal diffusivity and thermal conductivity

Thermal transport properties of pure oleic acid and composite samples i.e. thermal diffusivity and thermal conductivity are demonstrated in Fig. 3 and Fig. 4 at different testing temperatures. The error bars are added by using standard errors. Mass ratios of Al@C are selected from 0 to 1 wt% to compare its effect on the pure sample. Fig. 3 indicates that thermal diffusivities of different composite materials increase with the decrease of temperature, which also increase with mass ratio of Al@C. The highest thermal diffusivity could reach 0.256 mm^2·s^{-1} at 20°C and 1 wt% mass ratio of Al@C, which is improved by 88% when compared with that of pure sample. For different testing temperatures, thermal diffusivities of composite PCMs range from 0.165 mm^2·s^{-1} to 0.256 mm^2·s^{-1}. Thermal conductivities are then evaluated, and results demonstrate that a larger decreasing rate of thermal conductivity could be observed. This is mainly because densities of samples also decline sharply with the increase of the temperature. The results in reference (Chuah et al., 2006) are used for further calibration. It is worth noting that difference between testing and referential results is no more than 3%, which is within a reasonable range. For different temperatures, thermal conductivities of various composite oleic acids are in the range from 0.279 W·m^{-1}·K^{-1} to 0.452 W·m^{-1}·K^{-1}, which are improved by 51%-137% when compared with that of pure oleic acid. In order to have a comprehensive evaluation, thermal conductivities of composite oleic acid with 1 wt% mass ratio are compared by using other two common additives i.e. ENG and CNT as shown in Table 1. It is worth noting that

samples using ENG has the highest thermal conductivity. However, one striking fact is that phase separation happens by using ENG, which will deteriorate the performance after several working cycles (Cabeza et al., 2015). Thermal conductivity by using CNT shows the lowest value. Thus thermal conductivity of composite oleic acid using Al@C as additive has a reasonable performance, which is acceptable in real application. CNT and Al@C belong to nanoparticles, which should have good performance in developing composite materials.

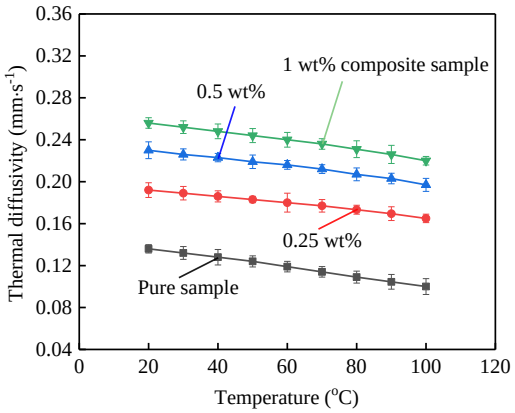

Fig. 3. Thermal diffusivities of samples vs. different testing temperatures.

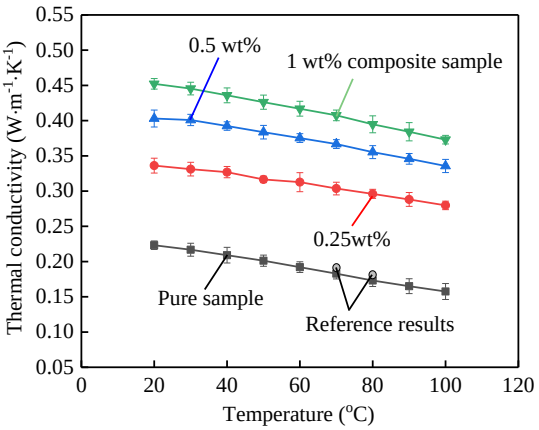

Fig. 4. Thermal conductivities of samples vs. different testing temperatures.

Table 1. Comparison of thermal conductivities of samples by using different additives.

Additive (1 wt%)	Thermal conductivity	Increment (pure)
ENG	0.51	1.51
CNT	0.38	1.16
Al@C	0.45	1.37

4.2. Viscosity

Viscosities of composite oleic acid are also tested at different temperatures by a viscometer, which are shown in Fig. 5. Results show that viscosities of different samples are quite close. Composite sample has a slightly higher viscosity than that of pure sample when testing temperature increases from 25°C to 40°C. Almost no difference could be observed when temperature is higher than 40°C. Al@C has a positive influence on viscosity in low temperature range. When testing temperature increases from 25°C to 75°C, dynamic viscosity decreases from 27.6 mPa·s to 4.9 mPa·s in terms of different samples. Arrhenius relationship is used to correlate the viscosity at different testing temperatures according to equation 5 (Soto et al., 2018). It could be transformed and linearly fitted by equation 6. Then activation energy and pre-experimental factor of composite oleic acid and pure sample are obtained as indicated in Table 2. Results demonstrate that pure sample has the higher activation energy and lower pre-experimental factor than composite sample. It is widely recognised that activation energy is within 15-30 $kJ \cdot mol^{-1}$ and natural logarithm of pre-experimental factor ranges from -17 Pa·s to -10 Pa·s in terms of low and moderate viscous fluids. Thus the fitting results of testing viscosity are in a reasonable range, and average absolute deviation of dynamic viscosity is no more than 5% when compared with ideal value calculated by each pure material according to Eyring equation (Franco and Nguyen, 2011).

$$\mu = A \cdot exp(E/RT) \tag{5}$$

where E is activation energy, A is pre-experimental factor and R is universal gas constant.

$$ln\mu = lnA + E/RT \tag{6}$$

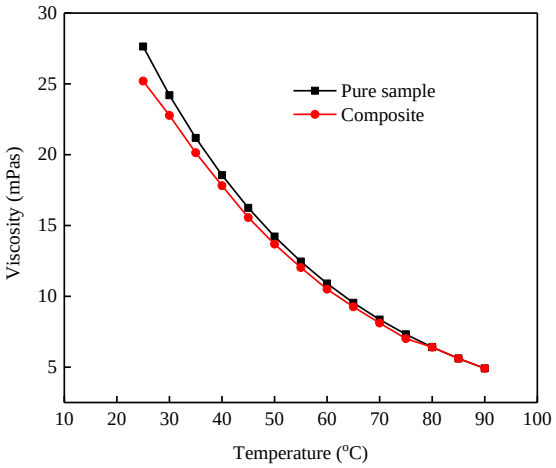

Fig. 5. Viscosity of pure and composite oleic acid vs different testing temperatures.

Table 2. Activation energy and pre-experimental factor of different samples.

Sample	ln(A) (Pa·s)	E (kJ·mol^{-1})
Pure	-13.2	23.9
Composite	-12.6	22.3

4.3. DSC testing

Phase change heat in the melting and freezing process are measured by a DSC. Since cold storage is concerned, the main research will focus on the freezing process which proceeds at a cooling rate of 1 K·min^{-1}. DSC curves of pure and composite oleic acid with 1 wt% of Al@C are shown in Fig. 6. Actually there is a distinct heat flow peak between the onset solidification temperature and end temperature. The peak heat flow is usually influenced by testing procedures, e.g. the peak heat flow in the phase change process will be lower when the heating rate becomes lower. Thus the onset temperatures are discussed as phase change temperature in this part. According to DSC curve, phase change temperature in freezing process ranges from 4^{o}C to 6^{o}C. Capric and lauric acid eutectic mixture with oleic acid in terms of different mass ratios could also be developed and selected for adjusting phase changing temperature for cold storage, which would satisfy the temperature range for a high temperature solar cooling application. Table 3 shows the main parameter of pure and composite oleic acid. Results demonstrate that phase change temperature of composite oleic acid is slightly changed from that of pure oleic acid due to the varied thermo-physical properties of composite samples. Latent heat of pure and composites in melting process are 137.1 kJ·kg^{-1} and 132.5 kJ·kg^{-1} with regard to total mass. Comparably, latent heat temperature of pure and composites in freezing process are 133.9 kJ·kg^{-1} and 129.1 kJ·kg^{-1}, respectively. To further understand the role of Al@C in composite PCM, different mass ratios of additive are used to compare their latent heats, which are shown in Fig. 7. It is demonstrated that latent heat of composite PCM in heating process is higher than that in cooling process. Latent heat of composite PCM decreases with the increase of Al@C. When mass ratio is higher than 0.5 wt%, latent heat begins to be stable. Also thermal stability is tested for 100 cycles, and the maximum deviation of latent heat is no more than 1%.

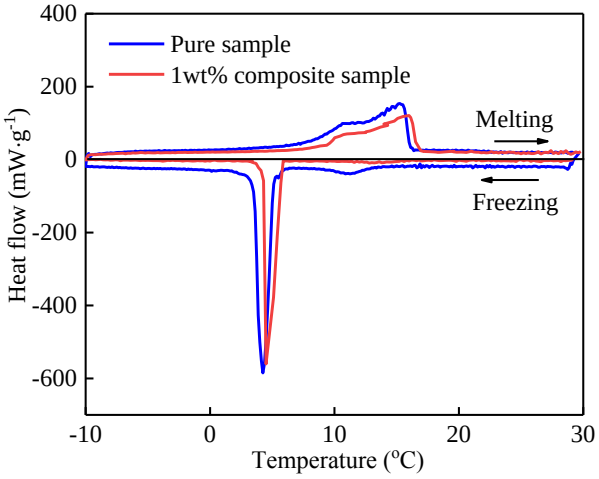

Fig. 6. DSC curves of pure and composite oleic acid.

Table 3 Characteristics of pure and composite oleic acid.

Testing	Sample	T_{onset} (°C)	Latent heat (kJ·kg^{-1})
Melting process	Pure	5.28	137.1
	Composite	5.77	132.5
Freezing process	Pure	6.94	133.9
	Composite	7.58	129.1

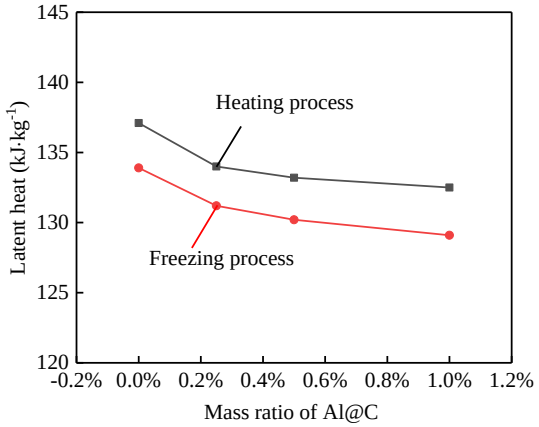

Fig. 7. Latent heats of samples in terms of different mass ratios of Al@C.

5. Possible application

5.1. System description

For solar cooling application, chilled water temperature of sorption system varies frequently under different external conditions. In order to further evaluate the performance of composite oleic acid for solar refrigeration, a

sorption system driven by solar energy is introduced as shown in Fig. 8a, which could refer to the references (Li et al., 2013; Li et al., 2015). Calcium chloride ($CaCl_2$)/activated carbon (AC) composite sorbents are used in this system, which has a rated cooling power of 2 kW. Both air conditioning condition and freezing condition could be realized since ammonia is used as working fluid. 20 m^2 evacuated tubes of solar collector are employed in this system with sun-tracking devices. Fig. 8b indicates the schematic of solar refrigeration system with auxiliary equipment, which mainly consists of a solar collector, a cooling tower, and a cold storage unit. The cold storage unit is filled with PCM capsules. Its diameter and wall thickness are the same with that in the reference (Cheng et al., 2016) i.e. effective length of cold storage unit, capsule diameter and wall thickness. The number of capsules is reduced to 100.

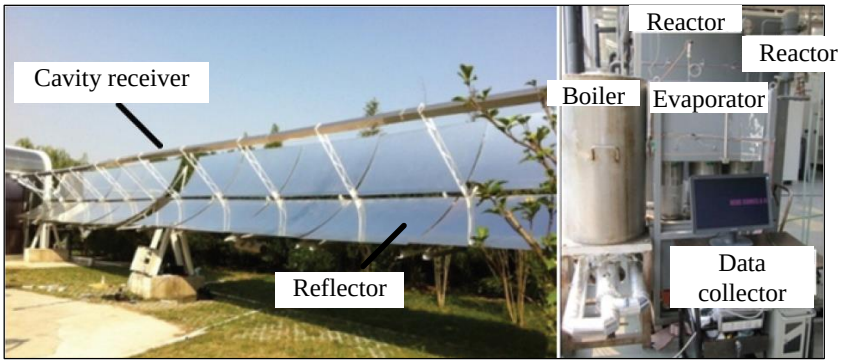

(a)

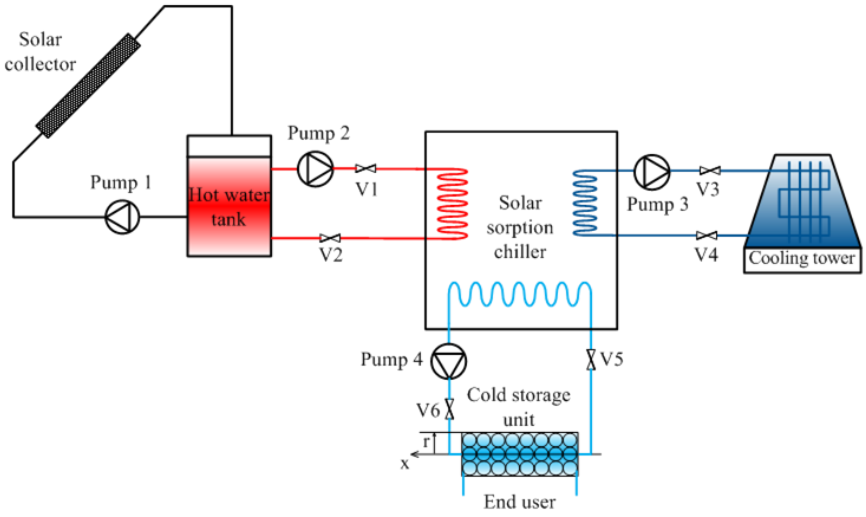

(b)

Fig. 8. The solar sorption refrigeration system (a) photo; (b) schematic of sorption chiller with cold storage unit (Li et al., 2013).

5.2. Mathematical model

For predicting the performance of cold storage unit, the coordinate for mathematical equation could refer to Fig. 8b. X axis represents the direction of HTF whereas r axis is for PCM. The mathematical model is based on the following assumptions: (1) Temperature and velocity gradient of cold storage unit in the radiant direction i.e. r axis are neglected. (2) Thermal resistance of spherical capsule wall could be overlooked; (3) Heat convection in the spherical capsules is neglected; (4) No cold leakage happens from the unit to the surroundings. The relevant governing equations are as follows:

Energy conservation equation could be expressed as equation 7.

$$\varepsilon\rho_f c_f\left(\frac{\partial T}{\partial t}+\mu\frac{\partial T}{\partial x}\right)=\lambda_f\frac{\partial^2 T_f}{\partial \mathrm{x}^2}+hS_p\left(T_{p|r=R}-T_f\right) \tag{7}$$

where ε represents void fraction of cold storage unit; T_f and T_p are temperatures of HTF and PCM; u is the mean velocity in the storage unit; S_p is the superficial capsule area. Heat transfer coefficient between HTF and PCM is then calculated according to the empirical method in reference (Smith, 1983):

Enthalpy method is employed for energy conservation equation of PCM capsules as equation 8.

$$\rho_p\frac{\partial H_p}{\partial t}=\lambda_p\frac{\partial^2 T_p}{\partial r^2}+\frac{2}{r}\lambda_p\frac{\partial T_p}{\partial r} \tag{8}$$

According to classical mixture rule, theoretical melting enthalpy of composite PCM can be calculated from equation 9.

$$\Delta H_{com}=\varphi\Delta H_{ole} \tag{9}$$

where ΔH_com is the phase change enthalpy of composite PCM; φ is mass fraction of Al@C; ΔH_ole is phase change enthalpy of pure sample.

The initial and boundary conditions for HTF and PCM are according to equations 10-15.

$$T_f(x,0)=T_{ini} \tag{10}$$

$$T_f(0,t)=T_{in} \tag{11}$$

$$T_f(0,t)=T_\mathrm{in} \tag{12}$$

$$\frac{\partial T_f(L,t)}{\partial x}=0 \tag{13}$$

where T_ini is phase change enthalpy of composite PCM; φ is the mass fraction of Al@C; ΔH_ole is phase change enthalpy of pure samples.

$$T_p(x,0) = T_{ini} \tag{14}$$

$$-\lambda_p \frac{\partial T_p}{\partial r} = h(T_{p|r=R} - T_f) \tag{15}$$

5.3. Dynamic solar chilled water temperature by using cold storage

A typical direct solar radiation data in summer from Shanghai meteorology database is adopted to predict the performance, which is shown in Fig. 9. The curves indicate the instantaneous radiation density from 7:00 am to 17:00 pm while the bars show the average value of each hour, which is used for desorption process of the reactor. The experiment is conducted from 10:00 to 16:00 on a clean summer day in Shanghai, China. The environmental temperature is 30°C and temperature for desorption of the reactor is 130°C. Based on these solar data, experimental chilled water outlet temperature of model sorption refrigeration system i.e. inlet temperature of cold storage unit could be obtained and its outlet temperature of the unit is then simulated.

These temperature variations i.e. chilled water outlet and cold storage unit outlet temperatures are indicated in Fig. 10. Both PCMs with Al@C and without Al@C are compared for further elaboration. It is extensively acknowledged that solar energy is an intermittent energy source which is variable between times and places. Also worth noting that sorption refrigeration is characterized as period and unstable output. Due to these dual reasons, the experimental chilled water outlet temperature in Fig. 10 has an obvious volatility. It initially decreases from 25°C to around 5°C when the reaction happens at 2 hour. Then the outlet temperature fluctuates and gradually increases in the end. Thus cold storage unit aims to stabilize the chilled water temperature while storing the cooling power. It is indicated that the outlet temperature of PCM unit almost remains stable when the time is close to 2 hour, which is quite conducive to solar driven cooling system. Besides, PCM with Al@C takes less time to be stable than that without using Al@C, which reveals a faster charging rate by using carbon nanoparticles due to its higher thermal conductivity. Actually charging rate is related with various factors e.g. effective length of cold storage unit and velocity of HTF. The aim of simulation in this part is to reveal the potentials of PCM for stabilizing the temperature and verify the effectiveness of Al@C. Besides, the average outlet temperature of composite PCM is a bit higher than that of pure samples, which may present more flexibilities. In real application, solar driven cooling system is better to be integrated with cold storage unit to stabilize the output temperature while storing the excessive cooling power. Cold storage is regarded as a modular unit and then multiple or cascaded cold storage concept could be applied if sufficient cold is supplied.

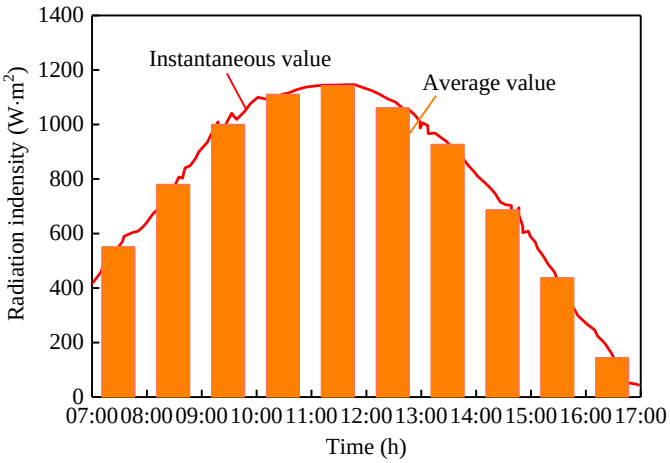

Fig. 9. A typical day direct solar radiation in Shanghai.

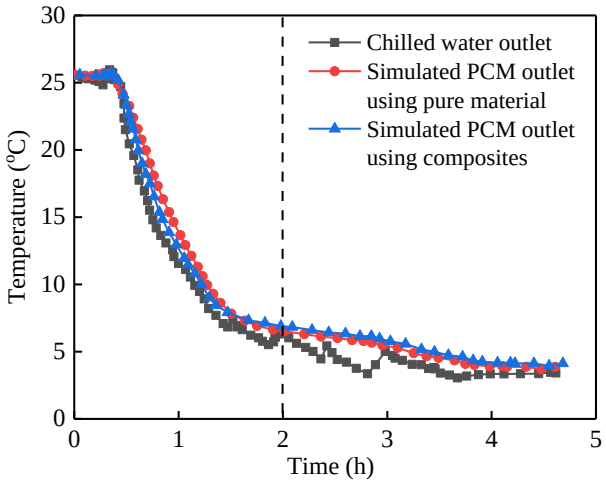

Fig. 10. Dynamic outlet temperature of chilled water.

6. Conclusions

In this paper, a novel composite oleic acid is developed with an additive of Al@C. Thermal conductivity and viscosity of composite samples are investigated and compared with pure sample. Phase change characteristics are also analyzed in terms of latent heat and onset temperature. Then a cold storage unit using PCM capsule is simulated for solar sorption cooling application. Conclusions are yielded as follows:

[1] Thermal diffusivities of different composite PCMs increase with the decrease of temperature and mass ratio of Al@C. The highest thermal diffusivity could reach 0.256 mm^2·s^{-1} at 20°C and 1 wt% mass ratio of Al@C, which is improved by 88% when compared with pure samples. For different testing

temperatures, thermal diffusivities of composite PCMs range from 0.165 $mm^2 \cdot s^{-1}$ to 0.256 $mm^2 \cdot s^{-1}$. Thermal conductivities of different composite samples are in the range from 0.279 $W \cdot m^{-1} \cdot K^{-1}$ to 0.452 $W \cdot m^{-1} \cdot K^{-1}$, which are improved by 51%-137% when compared with pure oleic acid.

[2] Composite sample has a slightly higher viscosity than pure sample when temperature increases from 25°C to 40°C , and almost no difference could be observed when temperature is higher than 40°C. When testing temperature increases from 25°C to 75°C, dynamic viscosities of different samples decrease from 27.6 mPa·s to 4.9 mPa·s.

[3] Phase change temperature in freezing process ranges from 4°C to 6°C, which could meet the temperature range for solar sorption cooling application. Phase change temperature of composite oleic acid is slightly changed from that of pure oleic. Phase change temperature of pure and composite samples in melting process and freezing process are 137.1 $kJ \cdot kg^{-1}$ and 132.5 $kJ \cdot kg^{-1}$ as well as 133.9 $kJ \cdot kg^{-1}$ and 129.1 $kJ \cdot kg^{-1}$, respectively. Latent heat of composite PCM decreases with the increase of Al@C.

[4] The experimental chilled water outlet temperature of solar sorption refrigeration system has an obvious volatility. The outlet temperature of PCM unit remains stable after 2 hour, which is quite conducive to solar driven sorption systems. The outlet temperature using PCM with Al@C takes less time to be stable than that without using Al@C. In real application, solar sorption cooling system is recommended to be integrated with cold storage unit.

Acknowledgements

This research was supported by National Natural Science Foundation of China under contract number (51606118), Innovative Research Groups under contract number (51521004), Heat-STRESS project (EP/N02155X/1) and Centre for Energy Systems Integration (EP/P001173/1) funded by Engineering and Physical Science Research Council of the UK.

References

Al-Alili, A., Hwang, Y., Radermacher, R., 2014. Review of solar thermal air conditioning technologies. International Journal of Refrigeration 39, 4-22.

Altohamy, A.A., Abd Rabbo, M.F., Sakr, R.Y., Attia, A.A.A., 2015. Effect of water based Al_2O_3 nanoparticle PCM on cool storage performance. Applied Thermal Engineering 84, 331-338.

Atinafu, D.G., Dong, W., Huang, X., Gao, H., Wang, G., 2018. Introduction of organic-organic eutectic PCM in

mesoporous N-doped carbons for enhanced thermal conductivity and energy storage capacity. Applied Energy 211, 1203-1215.

Barreneche, C., Ferrer, G., Palacios, A., Solé, A., Fernández, A.I., Cabeza, L.F., 2017. Empirical equations for viscosity and specific heat capacity determination of paraffin PCM and fatty acid PCM. IOP Conference Series: Materials Science and Engineering 251, 012114.

Cabeza, L.F., Barreneche, C., Martorell, I., Miró, L., Sari-Bey, S., Fois, M., Paksoy, H.O., Sahan, N., Weber, R., Constantinescu, M., Anghel, E.M., Malikova, M., Krupa, I., Delgado, M., Dolado, P., Furmanski, P., Jaworski, M., Haussmann, T., Gschwander, S., Fernández, A.I., 2015. Unconventional experimental technologies available for phase change materials (PCM) characterization. Part 1. Thermophysical properties. Renewable and Sustainable Energy Reviews 43, 1399-1414.

Chandrasekar, M., Suresh, S., Chandra Bose, A., 2010. Experimental investigations and theoretical determination of thermal conductivity and viscosity of Al_2O_3/water nanofluid. Experimental Thermal and Fluid Science 34, 210-216.

Chandrasekaran, P., Cheralathan, M., Kumaresan, V., Velraj, R., 2014a. Enhanced heat transfer characteristics of water based copper oxide nanofluid PCM (phase change material) in a spherical capsule during solidification for energy efficient cool thermal storage system. Energy 72, 636-642.

Chandrasekaran, P., Cheralathan, M., Kumaresan, V., Velraj, R., 2014b. Solidification behavior of water based nanofluid phase change material with a nucleating agent for cool thermal storage system. International Journal of Refrigeration 41, 157-163.

Cheng, X., Zhai, X., Wang, R., 2016. Thermal performance analysis of a packed bed cold storage unit using composite PCM capsules for high temperature solar cooling application. Applied Thermal Engineering 100, 247-255.

Chuah, T.G., Rozanna, D., Choong, T.S.Y., Sa'ari, M., Salmiah, A., 2006. Fatty acids used as phase change materials (PCMs) for thermal energy storage in building material applications. JURUTERA, 8-15.

Fang, X., Fan, L.-W., Ding, Q., Wang, X., Yao, X.-L., Hou, J.-F., Yu, Z.-T., Cheng, G.-H., Hu, Y.-C., Cen, K.-F., 2013. Increased Thermal Conductivity of Eicosane-Based Composite Phase Change Materials in the Presence of Graphene Nanoplatelets. Energy & Fuels 27, 4041-4047.

Franco, Z., Nguyen, Q.D., 2011. Flow properties of vegetable oil–diesel fuel blends. Fuel 90, 838-843.

Han, G., Fang, Z., Chen, M., 2010. Modified Eyring viscosity equation and calculation of activation energy based on the liquid quasi-lattice model. Science China Physics, Mechanics and Astronomy 53, 1853-1860.

Hussain, S.I., Dinesh, R., Roseline, A.A., Dhivya, S., Kalaiselvam, S., 2017. Enhanced thermal performance and study the influence of sub cooling on activated carbon dispersed eutectic PCM for cold storage applications. Energy and Buildings 143, 17-24.

Jiang, L., Lu, Y.J., Tang, K., Wang, Y.D., Wang, R., Roskilly, A.P., Wang, L., 2017. Investigation on heat and mass transfer performance of novel composite strontium chloride for sorption reactors. Applied Thermal Engineering 121, 410-418.

Jiang, L., Wang, L.W., Wang, R.Z., 2014. Investigation on thermal conductive consolidated composite $CaCl_2$ for adsorption refrigeration. International Journal of Thermal Sciences 81, 68-75.

Jiang, L., Xie, X.L., Wang, L.W., Wang, R.Z., Wang, Y.D., Roskilly, A.P., 2018. Investigation on an innovative sorption system to reduce nitrogen oxides of diesel engine by using carbon nanoparticle. Applied Thermal Engineering 134, 29-38.

Kumaresan, V., Chandrasekaran, P., Nanda, M., Maini, A.K., Velraj, R., 2013. Role of PCM based nanofluids for energy efficient cool thermal storage system. International Journal of Refrigeration 36, 1641-1647.

Li, C., Wang, R.Z., Wang, L.W., Li, T.X., Chen, Y., 2013. Experimental study on an adsorption icemaker driven by parabolic trough solar collector. Renewable Energy 57, 223-233.
Li, C., Yan, T., Wang, R., Wang, L., Li, T.X., Li, X., Lin, M., Xie, W.T., 2015. An experimental investigation of an adsorption ice-maker driven by parabolic trough collector. Heat transfer research 46, 347-368.
Li, G., Hwang, Y., Radermacher, R., 2012. Review of cold storage materials for air conditioning application. International Journal of Refrigeration 35, 2053-2077.
Lin, Y., Jia, Y., Alva, G., Fang, G., 2018. Review on thermal conductivity enhancement, thermal properties and applications of phase change materials in thermal energy storage. Renewable and Sustainable Energy Reviews 82, 2730-2742.
Merlin, K., Soto, J., Delaunay, D., Traonvouez, L., 2016. Industrial waste heat recovery using an enhanced conductivity latent heat thermal energy storage. Applied Energy 183, 491-503.
Miró, L., Gasia, J., Cabeza, L.F., 2016. Thermal energy storage (TES) for industrial waste heat (IWH) recovery: A review. Applied Energy 179, 284-301.
Oró, E., de Gracia, A., Castell, A., Farid, M.M., Cabeza, L.F., 2012. Review on phase change materials (PCMs) for cold thermal energy storage applications. Applied Energy 99, 513-533.
Pan, Q.W., Wang, R.Z., 2018. Study on operation strategy of a silica gel-water adsorption chiller in solar cooling application. Solar Energy.
Pantelic, J., Schiavon, S., Ning, B., Burdakis, E., Raftery, P., Bauman, F., 2018. Full scale laboratory experiment on the cooling capacity of a radiant floor system. Energy and Buildings 170, 134-144.
Sathishkumar, A., Kumaresan, V., Velraj, R., 2016. Solidification characteristics of water based graphene nanofluid PCM in a spherical capsule for cool thermal energy storage applications. International Journal of Refrigeration 66, 73-83.
Sidik, N.A.C., Kean, T.H., Chow, H.K., Rajaandra, A., Rahman, S., Kaur, J., 2018. Performance enhancement of cold thermal energy storage system using nanofluid phase change materials: A review. International Communications in Heat and Mass Transfer 94, 85-95.
Smith, J.M., 1983. Heat and mass transfer in packed beds, AIChE Journal 29, 1055-1055.
Soto, F., Alves, M., Valdés, J.C., Armas, O., Crnkovic, P., Rodrigues, G., Lacerda, A., Melo, L., 2018. The determination of the activation energy of diesel and biodiesel fuels and the analysis of engine performance and soot emissions. Fuel Processing Technology 174, 69-77.
Veerakumar, C., Sreekumar, A., 2016. Phase change material based cold thermal energy storage: Materials, techniques and applications – A review. International Journal of Refrigeration 67, 271-289.
Wang, R.Z., Pan, Q.W., Xu, Z.Y., 2016. 12 - Solar-powered adsorption cooling systems, Advances in Solar Heating and Cooling. Woodhead Publishing, pp. 299-328.
Yu, N., Wang, R.Z., Wang, L.W., 2013. Sorption thermal storage for solar energy. Progress in Energy and Combustion Science 39, 489-514.
Zhai, X.Q., Wang, X.L., Wang, T., Wang, R.Z., 2013. A review on phase change cold storage in air-conditioning system: Materials and applications. Renewable and Sustainable Energy Reviews 22, 108-120.
Zhao, K., Liu, X.-H., Jiang, Y., 2014. On-site measured performance of a radiant floor cooling/heating system in Xi'an Xianyang International Airport. Solar Energy 108, 274-286.
Zhao, R., Zhao, L., Wang, S., Deng, S., Li, H., Yu, Z., 2018. Solar-assisted pressure-temperature swing adsorption for CO_2 capture: Effect of adsorbent materials. Solar Energy Materials and Solar Cells 185, 494-504.